SCIENTIFIC REPORTS

OPEN

Eco-evolutionary Red Queen dynamics regulate biodiversity in a metabolite-driven microbial system

Received: 16 August 2017
Accepted: 29 November 2017
Published online: 15 December 2017

Juan A. Bonachela[1,3], Meike T. Wortel[2] & Nils Chr. Stenseth[2]

The Red Queen Hypothesis proposes that perpetual co-evolution among organisms can result from purely biotic drivers. After more than four decades, there is no satisfactory understanding as to which mechanisms trigger Red Queen dynamics or their implications for ecosystem features such as biodiversity. One reason for such a knowledge gap is that typical models are complicated theories where limit cycles represent an idealized Red Queen, and therefore cannot be used to devise experimental setups. Here, we bridge this gap by introducing a simple model for microbial systems able to show Red Queen dynamics. We explore diverse biotic sources that can drive the emergence of the Red Queen and that have the potential to be found in nature or to be replicated in the laboratory. Our model enables an analytical understanding of how Red Queen dynamics emerge in our setup, and the translation of model terms and phenomenology into general underlying mechanisms. We observe, for example, that in our system the Red Queen offers opportunities for the increase of biodiversity by facilitating challenging conditions for intraspecific dominance, whereas stasis tends to homogenize the system. Our results can be used to design and engineer experimental microbial systems showing Red Queen dynamics.

In its original formulation, the Red Queen Hypothesis proposes that co-evolution among co-existing species can be perpetual, with no need for abiotic factors to sustain it[1]. Stripping the Red Queen (RQ) from some of its original controversial constraints (e.g. "zero sum rule"[1–3]) leads to a generic scenario in which evolutionary changes in one species impose selection pressures on others that necessarily adapt in order to avoid extinction; this response in turn influences the first species, thus generating dynamic fitness landscapes perpetually altered by the reciprocal evolutionary responses of interacting species[4].

This less restrictive reading of the RQ Hypothesis has opened the door to interpreting a wider spectrum of situations as RQ dynamics. For example, although the original formulation intended to describe a macroevolutionary motif, the RQ is used to describe both macroevolutionary and microevolutionary patterns[2,3,5]. On the other hand, although the requirement for perpetual evolutionary "running" was initially interpreted as unbounded evolution (e.g. "arms race"), the RQ is currently also identified with co-evolutionary oscillations. In these oscillations, the evolutionary gradient experienced by one species changes sign due to the other co-evolving organisms, thus triggering a shift in the directional change of the focal adaptive traits[6].

From a theoretical point of view, some degree of ecological asymmetry is required for models to show evolutionary oscillations[7]. Theories typically seek to find the conditions for evolutionary limit cycles (labeled as RQ dynamics) as opposed to evolutionarily stable strategies (ESS), which are identified with stasis[8]. However, in these models it is often difficult to realize when exactly these RQ oscillations are driven by evolutionary responses of the species involved, as the RQ really requires, or are instead caused by ecological components. The reason is that, in most cases, oscillations in the adaptive trait are linked to population-density oscillations[9,10]. In such cases, the co-evolving species alternate dominance unceasingly, i.e. one species rises and forces a simultaneous decline of the rest of the species' densities; the RQ is identified as periodic changes in the relative frequency of the species involved, facilitating a winner-less scenario in which all species coexist. From this perspective, the RQ oscillations contribute to maintaining biodiversity[10]. Similarly, other models pinpoint the RQ as the cyclic alternation between a discrete number of strategies for finite populations using game-theory frameworks[11,12], or as

[1]Marine Population Modeling Group, Department of Mathematics and Statistics, University of Strathclyde, Glasgow, G1 1XH, Scotland, UK. [2]Centre for Ecological and Evolutionary Synthesis (CEES), Department of Biosciences, University of Oslo, PO Box 1066 Blindern, Oslo, 0316, Norway. [3]Present address: Department of Ecology, Evolution, and Natural Resources, 14 College Farm Rd, New Brunswick, NJ 08901, USA. Correspondence and requests for materials should be addressed to J.A.B. (email: juan.bonachela@rutgers.edu)

oscillations in the relative frequencies of alleles, with no need to keep track of population dynamics[13]. Moreover, models that show evolutionary oscillations in the adaptive traits' value often impose very specific multi-parameter functional forms linking the species interaction strengths with the also-assumed dynamics for the adaptive trait (e.g. seminal[8,14], or more complicated examples[9]). This specificity and required knowledge about the links between evolutionary and ecological dynamics contribute to a disconnect that prevents models from helping in the conception of experimental setups able to show RQ dynamics; for instance, because it may be difficult to match real traits or environmental conditions with model parameters and functions, or to find systems that fulfill such functional-response constraints. An experimental setup informed by and devised using models enables the understanding of fundamental aspects of the emerging experimental RQ dynamics such as the (ecological or evolutionary) mechanisms underlying such oscillations.

Here, we aim to fill this gap by studying a simple, generic model for microbial evolution able to show eco-evolutionary RQ oscillations. Based purely on biotic interactions, our model keeps track of each phenotype's population dynamics but, differently from the traditional approach, RQ dynamics are not linked to nor do they result from population-density oscillations. In our model, intraspecific competition for resources drives interspecific ecological interactions among generic bacterial strains which, in turn, influence the evolutionary target imposed by intraspecific competition. This feedback loop triggers a perpetual change of the fitness landscape that gives rise to eco-evolutionary RQ dynamics. For the sake of concreteness, we focused on a specific theoretical scenario in which genetic engineering and metabolic byproducts were used to achieve the necessary chain of interactions, but the mechanisms presented here are general. We employed a generic functional dependence between intra- and interspecific interactions that allowed us to explore different drivers for the RQ in such a scenario. We explored how these different drivers alter the emergent RQ dynamics, and studied the role of the RQ in biodiversity regulation. Our model allows for a theoretical understanding of key aspects of the RQ, providing information about the triggering mechanisms and systems susceptible to show evolutionary oscillations in the lab and the real world.

Methods

Microbial model. We assume a system composed of several strains of a generic microbial unicellular organism and allow for intraspecific variability, i.e. multiple phenotypes per strain. Phenotypes within a strain interact via intraspecific resource competition, one of the most basic ecological interactions[15]. In addition, strains are connected by an interspecific interaction to be specified. Because interspecific interactions may contribute to destabilizing an interconnected system and lead to its collapse[16], we set up a self-regulating interaction chain (an interspecific non-transitive cycle) to facilitate the survival of the strains.

Intraspecific dynamics. We assume continuous cultures (i.e. chemostat conditions) and, therefore, the dynamics of the number of cells for any phenotype i, N_i, are given by:

$$\frac{dN_i}{dt} = (\mu_i - w)N_i, \tag{1}$$

where μ represents growth rate, and w is the dilution rate of the chemostat (only source of mortality, assuming that cell death rates are negligible compared to dilution). See Table S1 for list of symbols and units. Strains in the system are differentiated only by the resource they grow on, which prevents interspecific competitive exclusion. Experimentally, this can be achieved by using knock-out techniques for the genes that control the assimilation of the discarded resources. Thus, only the S phenotypes that belong to each individual strain compete for the same single resource. The dynamics for the availability of the strain-a-specific resource A, $[A]$, are given by:

$$\frac{d[A]}{dt} = w\left([A]_{input} - [A]\right) - \sum_{i=1}^{S_a} N_i \mu_i / Y_a, \tag{2}$$

(and similarly for strains b, c… and their respective resources, B, C, etc.). The first term represents the inflow and outflow of nutrients, and the second term represents the uptake of nutrient A by all the S_a phenotypes (N_i cells per phenotype i). The nutrient intake is assimilated as growth with a constant yield factor Y_a and, therefore, we can refer indistinctly to uptake or growth. We assume that the latter is given by the simple Monod formulation[17]; if phenotype i belongs to strain a:

$$\mu_i = R(y)\frac{\mu_{max_i}[A]}{K_i + [A]}, \tag{3}$$

where μ_{max_i} represents the associated maximum growth rate, K_i the half-saturation constant, and $R(y)$ the interspecific interaction term.

Interspecific interactions. We encode the effect that any possible interspecific interaction has on growth using the effective function, $R(y)$, which depends on a driving biotic factor, y. Although not strictly necessary (see Supplementary Information, section S. VIII), we assume that this function is bounded and positively correlated with the biotic driver. For example, to describe the effect of strain c on phenotypes from strain a (Fig. S1):

$$R_a(y_c) = \frac{R_{top}}{1 + e^{-k_R\left(y_c - y_{ref}\right)}} + R_{min}. \tag{4}$$

R_{min} defines the minimum value for R, and the maximum value is given by $R_{max} = R_{top} + R_{min}$. The sensitivity of the interaction to the driver is provided by k_R and y_{ref}, which control slope and location of the R curve respectively, and depend on the specifics of the biotic factor y. As indicated in S. IV, these are the only free parameters of the model.

Non-transitive cycle. To set up the non-transitive cycle, an odd number of strains is required, and interspecific interactions need to be pairwise, directed, and negative: assuming 3 strains, a inhibits b; lower b growth benefits c; higher c growth in turn inhibits a, and so on. In such a chain, the directional change in a that initiates the cycle is reverted after one iteration (i.e. when c affects a), thus regulating and constraining interspecific interactions (see Fig. S2). Due to the positive role of R in cell growth (Eq. (3)), inhibition here means a decrease in R.

Specific example and drivers. For the sake of concreteness, we focus on the bacterium *Escherichia coli* hereon. We assume that each strain synthesizes and excretes two metabolic byproducts that, in combination, inhibit totally or partially the growth of one and only one of the other strains: strain c's inhibitor ratio only affects strain a phenotypes, a excretes inhibitors that can only be taken up by b, and c is the only strain affected by b-excreted inhibitors, achieving in this way the non-transitive cycle described in Fig. S2. Compound effects of metabolites have been reported such as the wild- *E. coli* growth-inhibition effect of valine requiring also isoleucine in a ratio 0.03:1[18,19], and ratiometric sensors have been engineered in the past for *E. coli*[20]. Inspired by, e.g. the positive correlation between *E. coli* cell growth and excretion of the inhibitor acetate[21], here good growth performance from a phenotype increases its metabolite ratio and therefore increases inhibition for the target strain. Thus, we assume that the biotic factor driving the interaction depends on growth efficiency, negatively correlated with the growth half-saturation constant (see Eq. (3)). For example:

$$y_c = \frac{K_c}{K_{ref_c}}. \tag{5}$$

Higher growth efficiency from c (i.e. lower K_c) reduces $R_a(y_c)$ and, therefore, a's growth. With no loss of generality, we use as representative K for the strain that of the dominant phenotype, typically overpowering the population average. To facilitate comparison across drivers, we use a normalization factor provided by the trade-off existing between the half-saturation constant and maximum growth rate (see below). Another plausible driver considers the relative growth efficiency (e.g. the inhibitory effect of the metabolite ratio is more noticeable if the target strain's growth performance is already low):

$$y = \frac{K_c}{K_a}, \tag{6}$$

Additional possible representatives for growth efficiency, and other biotic factors that can drive the interaction described above, are discussed in S. VI.

Adaptive traits. Byproduct synthesis and excretion can be physiologically cheap[22], and affect negligibly the survival probability of the producer strain, whereas intraspecific competition, always present, shapes the long-term behavior of the phenotypes. The latter is, therefore, the main source of evolutionary pressure on each phenotype in our system. Because the maximum growth rate and the half-saturation constant drive competition, we assume that each phenotype i is characterized by μ_{max_i} and K_i (only adaptive traits), with its primary resource indicating which strain the phenotype belongs to. Both traits are linked by a trade-off, $\mu_{\max_i} = \mu_{ref}\frac{\ln(K_i/K_{ref})}{\ln(K_i/K_{ref})+1}$, where μ_{ref} and K_{ref} are constants[23]. The yield factor, Y, does not play any role in the competitive ability of the organism and fitness; for simplicity, we assume that Y is identical for all strains. See S.I for more details.

Eco-evolutionary simulations. The ecological dynamics in our 3-strain system consist of the intraspecific interactions (Eqs (1)–(2)), coupled across strains through a non-transitive cycle via R (Eq. (4)) and the chosen driver, y. The evolutionary dynamics result from random mutations within each strain, which generate new phenotypes (new populations within the strain that differ in the value of the adaptive trait)[24,25]. Each phenotype's mutation probability depends on a mutation rate as well as the number of individuals per generation.

Starting from one single phenotype population per strain, mutant phenotypes enter the system at random times during the ecological dynamics. Intraspecific competition drives some phenotypes to extinction whereas other mutant phenotypes are created, triggering a succession of dominant phenotypes that approaches an evolutionarily stationary state (ESS) for each strain[6,26]. Focusing on, e.g. strain a, such ESS (Eqs (S4)–(S5)) is an evolutionary target that will remain constant for as long as the performance of c, which controls y_c and therefore R_a, does not change significantly. Therefore, trait evolution affects the interaction among strains which, in turn, affects cell growth, defining an eco-evolutionary feedback loop.

To ensure equivalent initial conditions for all drivers we studied, we used an initializing period of ~1000 days in which we impose $R = 1$ to lead all iterations of the system to a same initial stationary state; after that period, R becomes dynamic (Eq. (4)). This initialization method does not influence the outcome of the simulation.

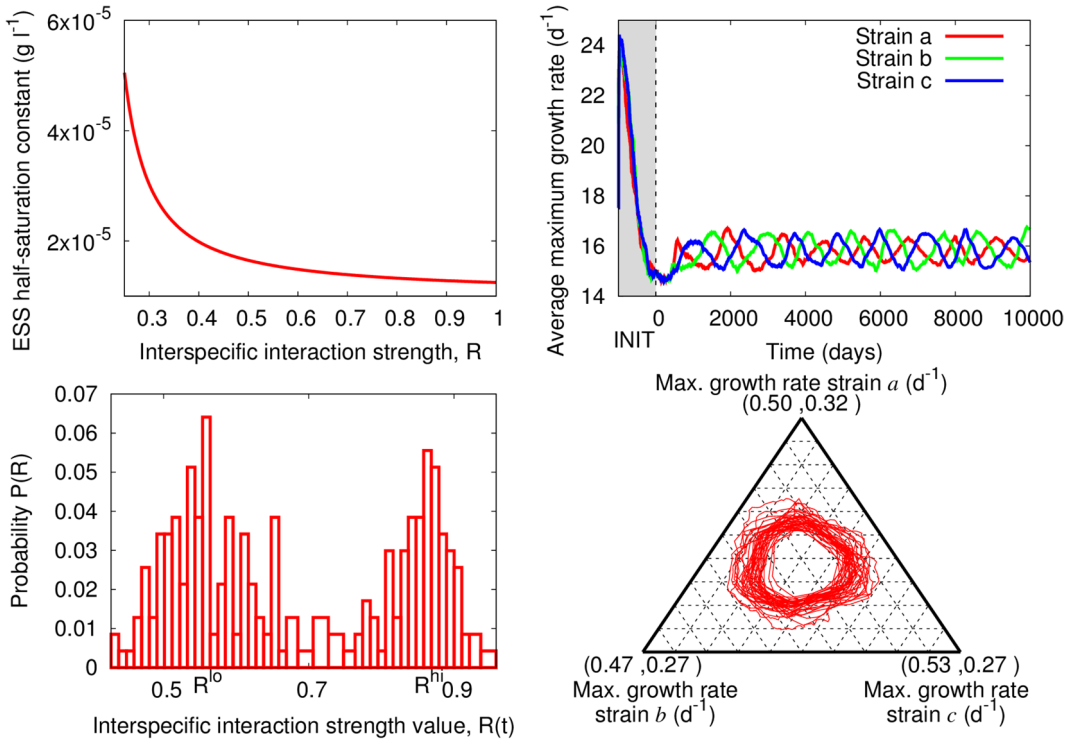

Figure 1. *K*-dependent biotic driver, Eq. (5). Upper Left: Dependence of the half-saturation constant that minimizes resource requirement (i.e. the ESS, Eq. (S5)) on the interaction strength, *R*. Upper Right: RQ dynamics emerging from the 3-strain dynamics when $k = 5$ and $y_{ref} = 2.5$, shown for the μ_{max} of the average phenotype within the strain (shaded area: initialization period). Lower Left: Probability distribution for *R*, showing bimodality with peaks around R^{lo} and R^{hi}. Lower Right: Ternary plot showing the normalized value of the average adaptive trait for the three strains, after removing the initial transient.

Evolutionary lag and biodiversity measures. The producer strain is a key part of the target strain's environment. Thus, evolutionary changes for the producer strain result in changes in the evolutionary target (or potential ESS) for the target strain. To quantify how challenging the new environment is for the target strain's phenotypes (and, therefore, the strength of the selection pressure), we use the evolutionary lag[4], or relative difference between the strain's trait value and the ESS. For the maximum growth rate, $L_{\mu_{max}}(t) = 1 - \frac{\mu_{max}(t)}{\mu_{max_{ESS}}(R(t))}$, (with the denominator provided by Eq. (S5). The emergence of RQ dynamics can affect also the strain number[4], (which changes with time), $S(t)$. We monitor these observables as well as the genetic diversity present in the ecosystem. Because we assume that phenotypic differences have only a genetic origin, we refer indistinctly to genotype and phenotype. We use three different biodiversity measures, namely the Shannon index (I_{Sh}, Eq. (S16)), and the standard deviation (I_{stdev}) and inter-quartile range (I_{IQR}) of the adaptive trait distribution (the latter defined as the weighted probability distribution of trait values present within each strain at each time).

Results

In the theoretical system proposed here, each strain's evolutionary target (or potential ESS) is given by the phenotype with the minimum resource requirement; resource requirement is inversely correlated with fitness and, therefore, it is a measure of competitive ability[26] (Fig. S3, left). This target, Eq. (S5), is influenced by the effect of the interspecific interaction, encoded in *R*. Larger *R* values select for phenotypes that require a smaller amount of nutrient. These phenotypes show also an enhanced growth efficiency, i.e. smaller *K* (Fig. 1 upper left panel, and Eq. (S1)), which allows cells to reach their maximum growth potential for smaller nutrient concentrations. These results are independent from the specific functional form for *R* (see analytical calculations in S. II). Due to the dynamic nature of the interspecific interaction, however, this target may or may not be realized. The latter case leads here to the RQ.

For drivers like Eq.(5), and with the help of the recursive method explained in S. V, we explored the areas of the (k_R, y_{ref}) space for which an ESS is reached and those in which RQ dynamics emerge (Fig. S3, right, Fig. S4, left, and Fig. 1, upper right). Different normalization factors for the driver altered the location of the RQ zones of the parameter space. These trait oscillations are shown in Fig. 1 for the maximum growth rate, μ_{max}, using the parametrization from Table 1. We show this adaptive trait as representative of the evolutionary dynamics because, due to the existing trade-off (Eq. (S1)), the results for *K* are qualitatively identical. The emerging RQ dynamics were identified as oscillations in the intraspecific average value for the adaptive trait. The oscillations for the 3 strains were correlated, connected through the interspecific interaction via the *R* function (in Fig. 1, driven by growth efficiency), which repeatedly visited R^{lo} and R^{hi}, effective minimum and maximum values for the interaction

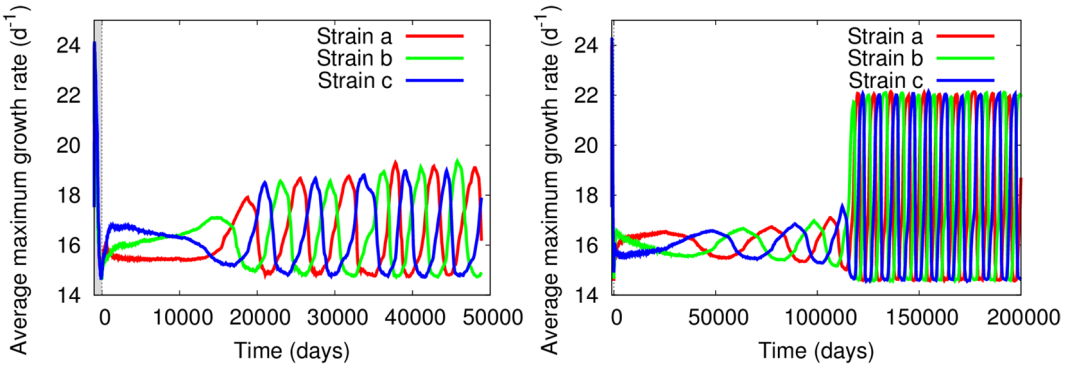

Figure 2. RQ dynamics driven by pairwise drivers with $k_R = 10$ and $y_{ref} = 1$. Left: Biotic driver y given by the ratio of maximum growth rates, Eq. (S9). Right: Driver provided by the relative affinity, Eq. (S10), showing a 10^5 day transient; other replicates show shorter or longer transients to reach the same stationary RQ oscillations.

strength (Fig. 1, lower-left panel). These recurring changes in the average trait value matched alternations in dominance occurring within each strain suggesting that, at each time, the corresponding dominant phenotype was overwhelmingly represented in the population (Fig. S4, right). Because strains explore the phenotypic space via mutations, the resulting RQ oscillations were irregular (Fig. 1, lower-right panel). In addition, different drivers generated different R^{lo} and R^{hi}, values that determined the amplitude of the oscillations (i.e. ranges of possible ESS values, see Fig. 1, upper left). These RQ dynamics were not accompanied by population-density oscillations or synchrony (Fig. S5). Population densities fluctuated stochastically around a stationary value in which an increase in density for one strain was not necessarily linked to a decrease in the density of any of the remaining strains. On the other hand, biotic drivers that depend on any of the rapidly-changing variables such as nutrient availability or population number (Eqs (S13)–(S15)) led to a rapidly-changing R function that generated oscillations for the ecological variables (e.g. N_i) but not for the adaptive traits. For the latter drivers, the traits reached stasis. RQ oscillations could be recovered in these cases, however, when longer periods (e.g. several days) were imposed for changes in such biotic driver (not shown).

For all pairwise biotic drivers (Eqs (6), (S9) and (S10)), fixing generically $y_{ref} = 1$ (i.e. equal performance for both strains) and the shape/asymmetry parameter to the intermediate value $k_R = 10$ led to RQ dynamics (Fig. 2); low values for k_R led to stasis. Oscillations triggered by these drivers showed a very heterogeneous timing. Different replicates of the same system showed hugely-different transients, sometimes as short as the initialization period and other cases requiring thousands of days to reach the stationary oscillations. In all cases, amplitudes during the initial transient were small and the associated period long, difficult to discern from stasis. The period of the oscillations progressively shortened while the amplitude increased until, eventually, stationary oscillations were reached. For some drivers, R^{lo} and R^{hi} and associated ranges for the adaptive traits were given by effective values different from the extreme ones (Fig. 2, left). For other pairwise drivers, RQ oscillations ranged any possible value for the trait allowed by the feasibility conditions, i.e. $R^{lo} = R_{min}$ and $R^{hi} = R_{max}$ (Fig. 2, right).

Both amplitude and period of the RQ oscillations showed a close link with the evolutionary lag, $L(t)$, and the number of phenotypes per strain, $S(t)$. For oscillations with long periods and small amplitude (e.g. long transients in Fig. 2), and for stasis, S grew monotonically with no apparent saturation (for the length of our simulations) and $L(t)$ stayed at a constant, low value (Fig. S6, left). This behavior was also observed during the initialization transient in all cases (Fig. S6 for $t < 1000$). When the RQ regime was reached, however, the number of phenotypes showed irregular oscillations formed by $S(t)$ increases followed by sharp declines, with the lag function showing spikes that matched dips in $S(t)$ and vice versa. For sufficiently-high lags, the decline in $S(t)$ led to the strain's extinction, breaking in this way the non-transitive cycle (Fig. S6, right panel). This collapse points to a mismatch between the strain's adaptation rate and the rate of change of its environment. We confirmed this hypothesis by running "rescue" simulations in which we introduced a phenotype matching the ESS when strains experienced large values of the lag. This evolutionary rescue instantaneously reduced lags to zero, thus allowing strains to stay in the system.

The phenomenology above suggests a close relationship between RQ oscillations and genetic diversity, I(t) (equivalently, phenotypic diversity, see Methods). Indeed, Fig. 3 (left panel) shows a coincidence between large variations in S, L, and I_{stdev}. Unexpectedly, a decrease in the number of phenotypes within the strain led to a peak in genetic diversity. To clarify this point, we monitored the changes in location and spread of the intraspecific genetic distribution. Figure 3 (right panel) shows boxplots for a representative time window taken from the left panel. Each box's height indicates the distance between first and third quartile for such distribution, with the median represented by the thick line within the box (whiskers represent the maximum and the minimum within the distribution). Periods with low lag showed very narrow distributions (thin boxes) heavily centered around a clear dominant phenotype; in turn, peaks in lag were associated with wide distributions with no clear dominant phenotype.

Different forms for the biotic driver and interspecific interaction strength function showed similar results (see S. VI and S. VIII).

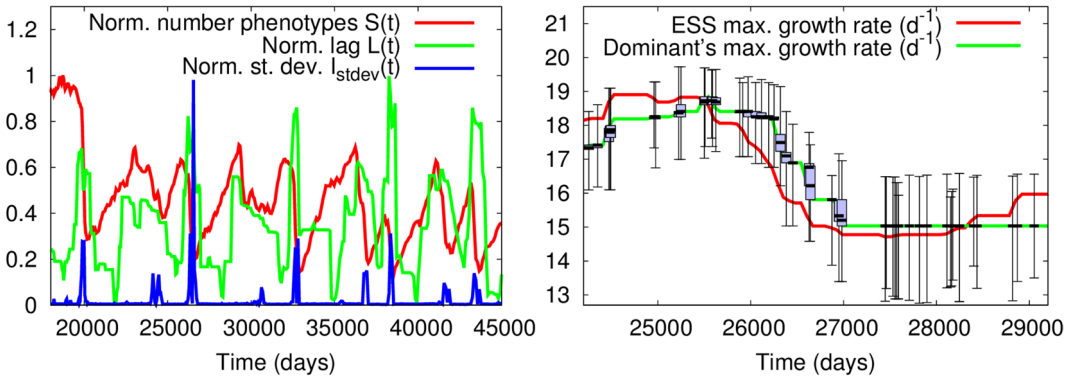

Figure 3. Detail of typical dynamics for a strain at the RQ regime. Left: Number of phenotypes per species, and lag and biodiversity for μ_{max}; to facilitate comparison, the three observables are normalized by their maximum value in that window. Right: Detail of the dynamics on the left panel, showing changes in genetic variability and distribution (box size) as a function of time.

Discussion

In stable environments, one single winner is expected when many different organisms compete for one single resource[26]. Moreover, there exists an optimal strategy able to outcompete any other phenotype, the ESS[27] (S. II). Here, we have used these well-known results to devise a generic system in which eco-evolutionary interactions generate RQ oscillations.

Evolution is manifested here as an intraspecific alternation in dominance through mutation and competition. Evolution affects a focal strain's growth efficiency and ratio of synthesized metabolic byproducts, thus altering the inhibition of a target strain's growth. A chain of such interspecific interactions forms an ecological non-transitive cycle through which, after the completion of the cycle, the focal strain's adaptation reverts its evolutionary gradient, closing in this way an eco-evolutionary feedback loop ultimately responsible for the RQ dynamics (Fig. 4). Therefore, these oscillations emerge from an indirect interaction between strains, as the evolution of the focal strain alters the environment of the target strain, which in turn triggers the target strain's adaptive response.

In our system, evolutionary oscillations are not accompanied by population density ones because the metabolite ratio availability, and not the metabolites per se, generates inhibition and correlates with the producer's growth performance/efficiency; there is an evolutionary driver for the ecological (non-transitive) interspecific interactions. Note that, although necessary to sustain them, the ecological non-transitive cycle does not suffice to generate these RQ oscillations (drivers such as, e.g. Eqs (S11–S15) do not show RQ dynamics although they show population density ones, as discussed below). The RQ emerges because the ecological non-transitive cycle affects the target strain's environment (and selection pressure) only after the producer strain has changed significantly and, with it, the biotic driver. In addition, upon completion of a cycle, evolutionary and ecological pressures push a strain in opposite directions, eventually giving rise to RQ oscillations (Fig. 4). On one hand, intraspecific evolution leads to increasing competitive ability within the strain by reducing resource requirement and half-saturation constant (and maximum growth rate, which sets a gleaner versus opportunist trade-off[28]). On the other hand, these smaller and smaller trait values translate into smaller and smaller R (higher inhibition), which in turn select for larger and larger values for those very same traits. RQ oscillations emerge from strains trying to reach those two changing evolutionary targets (imposed by R^{hi} and R^{lo}, Fig. 1 lower left panel). As an example, when strain a is subject to $R_a = R^{hi}$, evolution will lead its adaptive traits towards low values, thus reducing R_b to R^{lo}. In consequence, for strain b high values of the traits will be selected for, which will lead to $R_c = R^{hi}$ and, therefore, to low values for strain c's adaptive traits, resulting in $R_a = R^{lo}$. Thus, after the completion of the cycle, the evolutionary gradient for a is reverted (section S. III and Fig. S2).

Importantly, some time delay needs to be associated with this change of sign of the evolutionary gradient, as the strain requires time to explore the phenotypic space and generate sufficient genetic diversity to track significant changes in the evolutionary target. Because our drivers depend on the strain's representative value for the adaptive traits, significant changes in the driver only occur when there is an alternation in dominance. Note that, because the dominant is also the most abundant phenotype within the strain, experiments sampling the population to measure each strain's trait value should be able to observe these RQ dynamics.

A lack of a delay is precisely the reason why we cannot observe RQ dynamics in biotic drivers that are too sensitive to changes in the environment (Eqs (S12)–(S15)). In these cases, quick changes in R happen in ecological time and therefore can be interpreted as acclimation responses that obviate the need for the population to adapt evolutionarily. The system tends towards an ESS that averages over time these fast changes in the fitness landscape.

Our results highlight the role of the RQ as key regulator of biodiversity across evolutionary scales. Differently from past work[10], biodiversity does not refer here to the number of coexisting strains, fixed in our system from the outset, but to the spread of the intraspecific trait distribution. Between changes in the evolutionary target, the phenotypes that are far from the ESS quickly go extinct as the constant environment selects for the fittest phenotypes. The dominant phenotype is found in such large numbers that most mutations result from this or close phenotypes, which can coexist for a considerably long time. Thus, the genetic distribution is heavily centered around the dominant genotype/phenotype while remaining long-tailed due to unusual mutants (thin boxes with

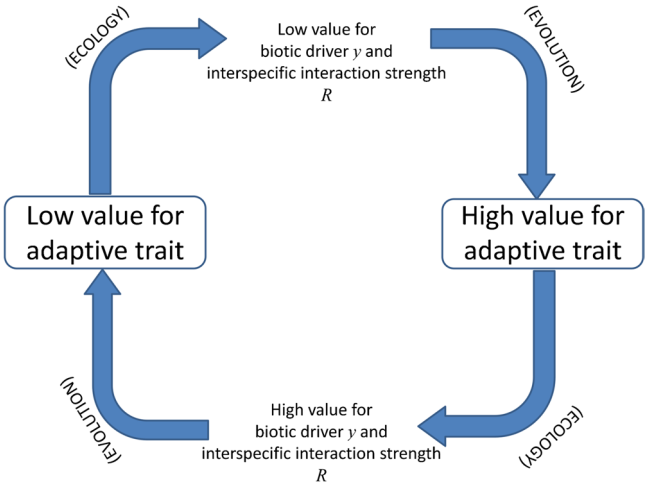

Figure 4. Summary of the eco-evolutionary feedback loop generating RQ dynamics.

long whiskers in Fig. 3, right panel). A change in the environment (i.e. change in R) sets a new evolutionary target, normally challenging enough (i.e. different enough from the previous ESS) to dethrone the ruling dominant and close phenotypes. As a measure of selection pressure, high lags indicate highly-challenging conditions for each phenotype within the strain. The larger the lag at the moment of change, the more dramatic the selection process. Thus, lag peaks match changes in ESS that trigger dominance alternation shortly after. RQ dynamics and associated changes in evolutionary target provide new phenotypes with the chance to thrive and replicate, challenging dominance. Without a clear dominant phenotype, the spread of the genetic distribution increases in transitional stages, reason why we observe the "paradoxical" decrease in the number of phenotypes per strain ($S(t)$) matching peaks in lag ($L(t)$) and biodiversity ($I(t)$). Conversely, S rises monotonically during periods in which the environment remains constant, but biodiversity does not increase because most of the new mutants will be phenotypically-close to the dominant. We propose that both S and L can be used as indicators of the emergence of RQ dynamics, which opens new and exciting possibilities to characterize the RQ in experiments.

In addition, RQ dynamics contribute to the resilience of the ecosystem. Environmental changes renew the adaptive landscape and constitute an opportunity for the creation of biodiversity. Biodiversity acts as a buffer that may allow the strain to respond to the changes in the evolutionary target imposed by the interspecific interaction. In consequence, long periods around the same ESS make the strain less resilient against environmental change due to the reduced genetic diversity.

Note that our RQ oscillations do not result from negative frequency dependence[29], as it is not "being rare" that matters but being different from the current dominant in the "right way". In spite of the peaks in biodiversity after a dominant goes extinct, the difference between previous and new environmental conditions can be too sharp (sudden large lag peaks) for the strain to "find" the right phenotype in time to avoid extinction. On the other hand, low lags accompany oscillations with low amplitude and period because the evolutionary process is generating enough genetic diversity for the strain to catch up quickly with such changes (e.g. low amplitudes observed in the transients of Fig. 2).

The irregular character of the amplitude and timing of our RQ oscillations stems from natural selection acting on phenotypes obtained from random mutations. For the biotic drivers Eq. (5) and (S7)–(S8), the amplitude is mostly determined by the parametrization of the R function, which determines the realized extremes R^{lo}, and R^{hi}. The variability in the transient observed for some pairwise biotic drivers (Eqs (6) and (S9)–(S10)) reflects the irregular, random way in which incipient RQ oscillations progressively increase in amplitude to reach the realized trait extremes (motivated by R^{lo} and R^{hi}). Such increase could result from a stochastic amplification of the oscillations, but without any analytical basis the underlying mechanism remains unclear.

We have focused, for the sake of concreteness, on one specific experimental realization. However, the basic principle underlying the RQ oscillations for our 3 bacterial strains is general. Our model suggests that natural or synthetic systems can show evolutionary oscillations even if species do not interact directly; it would suffice if one species' evolution alters negatively the environment of only the next species from a closed (odd) chain. Moreover, intraspecific competition drives each strain's evolution in our system, but any fitness-related changes/mechanisms may alternatively trigger the evolutionary cycle we identify here as the RQ. On the other hand, ecological non-transitive cycles like the one described here can be engineered in multiple ways in many microbial systems (see S. III). Because our RQ-inducing drivers depend on traits, lab strains should not lose the engineered mechanisms and, therefore, they need to be coupled to essential cell components. More generally, we propose that sufficiently-asymmetric drivers related to pairwise interactions as the ones described above generically trigger emergent RQ oscillations that self-organize to their maximum amplitude with no additional fine-tuning. In experiments, the R function and associated parameters will be heavily constrained by the type of biotic driver and interaction set up during the genetic engineering that produces the experimental layout. Different shapes and parameters for the interaction function R do not alter qualitatively the results above. Other parameters are

fixed by choices such as the duration or strength of the forcing period (which do not alter any of the results above, qualitatively or quantitatively), the dilution rate or resource input concentration (which constrain the feasibility conditions and the ranges for the trait amplitude in the RQ regime), or type of resource (which determines the yield factor, *Y*, and the trade-off reference values and form, just changing the target ESS for each strain and ranges for the RQ oscillations). We could have also considered drivers that are positively correlated with growth efficiency (e.g. focusing on growth-enhancing aminoacids excreted for optimal growth performance, S. III), in which case the non-transitive cycle would have required a negative correlation between the *R* function and the driver.

Ultimately, our theoretical framework can be used to predict whether a particular experimental setup will be able to show RQ dynamics, to inform such experiment and help in its design, and extend it to, e.g. longer time scales that cannot be achieved otherwise. Our model can also go beyond experiments studying aspects such as the strength of the evolutionary pressure (i.e. lag) and biodiversity. Our framework can indeed help discern whether associated experimental observables correspond to real versus apparent stasis; for example, RQ dynamics where the amplitude is small and the period long. We hope our work will inspire and inform experiments with which unravel the mysteries of the RQ.

References

1. Van Valen, L. A New Evolutionary Law. *Evol. Theory* **1**, 1–30 (1973).
2. Vermeij, G. J. & Roopnarine, P. D. Reining in the Red Queen: the dynamics of adaptation and extinction reexamined. *Paleobiology* **39**, 560–575 (2013).
3. Voje, K. L., Holen, Ø. H., Liow, L. H. & Stenseth, N. C. The role of biotic forces in driving macroevolution: beyond the Red Queen. *Proc. Roy. Soc. Lond. B* **282**, 20150186 (2015).
4. Stenseth, N. C. & Maynard Smith, J. Coevolution in Ecosystems: Red Queen Evolution or Stasis? *Evolution* **38**, 870–880 (1984).
5. Liow, L. H., Van Valen, L. & Stenseth, N. C. Red Queen: from populations to taxa and communities. *TREE* **26**, 349–358 (2011).
6. Brockhurst, M. A. *et al*. Running with the Red Queen: the role of biotic conflicts in evolution. *Proc. Roy. Soc. Lond. B* **281**, 2014.1382 (2014).
7. Nordbotten, J. M. & Stenseth, N. C. Asymmetric ecological conditions favor Red-Queen type of continued evolution over stasis. *Proc. Natl. Acad. Sci. USA* **113**, 1847–1852 (2016).
8. Marrow, P., Law, R. & Cannings, C. The Coevolution of Predator–Prey Interactions: ESSs and Red QueenDynamics. *Proc. Roy. Soc. Lond. B* **250**, 133–141 (1992).
9. Khibnik, A. I. & Kondrashov, A. S. Three mechanisms of Red Queen dynamics. *Proc. Roy. Soc. Lond. B* **264**, 1049–1056 (1997).
10. Rabajante, J. F. *et al*. Red Queen dynamics in multi-host and multi-parasite interaction system. *Sci. Rep.* **5**, 10004 (2015).
11. Damore, J. A. & Gore, J. A slowly evolving host moves first in symbiotic interactions. *Evolution* **65**, 2391–2398 (2011).
12. Veller, C., Hayward, L. K., Hilbe, C. & Nowak, M. A. The Red Queen and King in finite populations. *Proc. Nat. Acad. Sci. USA* **114**, E5396–E5405 (2017).
13. Agrawal, A. & Lively, C. M. Infection genetics: gene-for-gene versus matchin-alleles models and all points in between. *Evol. Ecol. Res.* **4**, 79–90 (2002).
14. Dieckmann, U., Marrow, P. & Law, R. Evolutionary cycling in predator-prey interactions: population dynamics and the Red Queen. *J. Theor. Biol.* **176**, 91–102 (1995).
15. Begon, M., Townsend, C.R. & Harper, J. L. *Ecology: From Individuals to Ecosystems*, (Blackwell Publishing 2006).
16. May, R. M. Will a Large Complex System be Stable? *Nature* **238**, 413–414 (1972).
17. Monod, J. Technique de Culture Continue. Theory et Applications. *Ann. Inst. Pasteur* **79**, 390–410 (1950).
18. De Felice, M., Levinthal, M., Iaccarino, M. & Guardiola, J. Growth inhibition as a consequence of antagonism between related amino acids: effect of valine in *Escherichia coli* K-12. *Microbiol. Rev.* **43**, 42–58 (1979).
19. Glover, S. W. Valine-resistant mutants of *Escherichia coli* K-12. *Genet. Res.* **3**, 448–460 (1962).
20. Daniel, R., Rubens, J. R., Sarpeshkar, R. & Lu, T. K. Synthetic analog computation in living cells. *Nature* **497**, 619–623 (2013).
21. Eiteman, M. A. & Altman, E. Overcoming acetate in *Escherichia coli* recombinant protein fermentations. *Trends Biotechnol.* **24**, 530–536 (2006).
22. Wintermute, E. H. & Silver, P. A. Emergent cooperation in microbial metabolism. *Mol. Sys. Biol.* **6**, 407 (2010).
23. Wirtz, K. W. A generic model for changes in microbial kinetic coefficients. *J. Biotech.* **97**, 147–162 (2002).
24. Bonachela, J. A. & Levin, S. A. Evolutionary Comparison Between Viral Lysis Rate and Latent Period. *J.Theor.Biol.* **345**, 32–42 (2014).
25. Lomas, M. W., Bonachela, J. A., Levin, S. A. & Martiny, A. C. Impact of ocean phytoplankton diversity on phosphate uptake. *Proc. Natl. Acad. Sci. USA* **111**, 17540–17545 (2014).
26. Tilman D. *Resource Competition and Community Structure* (Princeton University Press, 1982).
27. Dercole, F. & Rinaldi, S. *Analysis of Evolutionary Processes: the Adaptive Dynamics Approach and its Applications* (Princeton University Press, 2008).
28. Litchman, E., Klausmeier, C. A., Schofield, O. M. & Falkowski, P. G. The role of functional traits and trade-offs in structuring phytoplankton communities: scaling from cellular to ecosystem level. *Ecol. Lett.* **10**, 1170–1181 (2007).
29. Decaestecker, E. *et al*. Host-parasite "Red Queen" dynamics archived in pond sediment. *Nature* **450**, 870–874 (2007).

Acknowledgements

The authors would like to thank C. Caceres, E. De Muinck, B. Fischer, M. M. Liljegren, S. Levin, and P. Trosvik for helpful discussions, and M.A. Fortuna and M.A. Muñoz for critical reading of the manuscript. J.A.B. was supported by the Marine Alliance for Science and Technology for Scotland (MASTS) pooling initiative, funded by the Scottish Funding Council (HR09011) and contributing institutions. The authors acknowledge support from Nordforsk through the GreenMAR project, and from the Research Council of Norway through the Centre for Ecology and Evolutionary Synthesis.

Author Contributions

J.A.B., M.T.W., and N.C.S. designed research; J.A.B. performed research, developed the model, and wrote the article with input from M.T.W. and N.C.S.

Additional Information

Supplementary information accompanies this paper at https://doi.org/10.1038/s41598-017-17774-4.

Competing Interests: The authors declare that they have no competing interests.

Publisher's note: Springer Nature remains neutral with regard to jurisdictional claims in published maps and institutional affiliations.

Eco-evolutionary Red Queen dynamics regulate biodiversity in a metabolite-driven microbial system

Supplementary Information

Juan A. Bonachela*†[1], Meike T. Wortel[2], and Nils Chr. Stenseth[2]

[1]Marine Population Modeling Group, Department of Mathematics and Statistics, University of Strathclyde, Glasgow G1 1XH, Scotland,UK.
[2]Centre for Ecological and Evolutionary Synthesis (CEES), Department of Biosciences, University of Oslo, PO Box 1066 Blindern, Oslo 0316, Norway

S.I Trade-off function

The maximum growth rate, μ_{max_a}, and the half-saturation constant, K_a, are linked by a trade-off that depends on the type of microbe and resource it feeds upon. In our model, strains feed on different resources; however, due to the lack of information about the trade-off associated with different sugars (and to highlight the generality of our results), we use for all three strains the functional form for *E. coli* growing on glucose [1]:

$$\mu_{max_i} = \mu_{ref} \frac{\ln\left(K_i/K_{ref}\right)}{\ln\left(K_i/K_{ref}\right)+1} \tag{S1}$$

where μ_{ref} and K_{ref} are reference values that depend on the specific resource and species under study (see Table 1 for values used here). Our results do not depend qualitatively on the shape or parametrization of this trade-off as long as the trade-off holds, i.e. there is a positive link between the two traits. See S.VIII.

S.II Ecological and evolutionary steady state for intraspecific competition

Without loss of generality, let us focus on strain a hereon. In the model defined by equations Eq.(2)-(3), the chemostat conditions ensure reaching a stationary state, given by:

*To whom correspondence should be addressed: juan.bonachela@rutgers.edu
†Current address: Department of Ecology, Evolution, and Natural Resources, 14 College Farm Rd, New Brunswick, NJ 08901, USA.

$$[A]_{st} = \frac{w\, K_a}{R_a \mu_{max_a} - w} \tag{S2}$$

for the nutrient (note the feasibility condition $R_a \mu_{max_a} > w$), and:

$$N_{st} = Y_a \left([A]_{input} - [A]_{st} \right) \tag{S3}$$

for the population of cells.

Thus, if K (conversely, μ_{max}) is the only adaptive trait (see main text), and with competition as only possible interaction among different phenotypes of the focal strain a, the only possible result is one single dominant phenotype: the one that requires the least amount of resources [2], as competitive ability is inversely correlated with resource requirement. We can calculate this *evolutionarily stable strategy* (ESS) [3], by calculating the value of the adaptive trait that minimizes resources at the stationary state, that is:

$$\frac{d[A]_{st}}{dK_a} = 0;$$

Using Eq.(S1) and defining $z = \log\left(K_a / K_{ref}\right)$, the condition given by Eq.(S4) can be expressed as an equation for z whose solution is given by:

$$z^* = \frac{(2w - R_a \mu_{ref}) + \sqrt{\left(R_a \mu_{ref} - 2w\right)^2 + 4\left(R_a^2 \mu_{ref}^2 - w^2\right)}}{2\left(R_a \mu_{ref} - w\right)} \tag{S4}$$

(note the feasibility condition $R_a > 4w/(5\mu_{ref})$) and the ESS therefore can be written as:

$$\begin{aligned} \mu_{max_{a_{ESS}}} &= \mu_{ref} \frac{z^*}{z^* + 1} \\ K_{a_{ESS}} &= K_{ref} e^{z^*}. \end{aligned} \tag{S5}$$

The resource requirement is thus given by:

$$[A]_{st_{ESS}} = \frac{w\, K_{a_{ESS}}}{\mu_{max_{a_{ESS}}} - w} \tag{S6}$$

which depends on the adaptive traits and the dilution rate. Note that, following this equation the yield factor, Y, does not play any role in the competitive ability of the organism; z^* is mainly determined by the trade-off reference values, and by the environment (through the interspecific interaction strength and the dilution rate, biotic and abiotic factors respectively). Changes in R_a (in this case, triggered by strain c) will thus alter strain a's evolutionary target.

For a fixed R, the ESS above is also convergence-stable. Therefore, with one single strain the only possible long-term evolutionary outcome possible under chemostat conditions is an ESS, which can be interpreted as stasis and, therefore, opposite to Red Queen (RQ) dynamics.

S.III Non-transitive cycle

Our system prevents the collapse or divergence of the co-existing strains through an interspecific non-transitive cycle that is regulated/modified by the outcome of intraspecific competition for strain-specific resources. Such cycle can be engineered in many ways in the laboratory.

In the example discussed in the main text, good growth performance for, e.g. a (i.e. low y_a) leads to a high inhibitor ratio, which translates into a low $R_b(y_a)$ and the consequent reduction in strain b's growth. Such inhibition, in turn, gives rise to an evolutionary pressure selecting for lower growth performance for phenotypes belonging to strain b (high y_b) and, thus, low inhibitor ratio leading to a high $R_c(y_b)$) representing the lack of effect on strain c's growth. Thus, phenotypes from strain c can grow at a high rate, which facilitates high inhibitor ratios that will reduce strain a's growth, closing in this way the non-transitive cycle (see Fig.S2). After the completion of a period, the cycle can be summarized as a loop from the originating strain to itself, which can be seen in the figure by omitting the shaded area.

In addition to the examples outlined in the main text, there are many other possibilities to engineer cells to obtain such trait-based non-transitive cycle. For example, for *Bacillus subtilis* glutamate utilization requires the presence of arginine [4], another metabolic byproduct; or the cycle may be based on the use of byproducts that are synthesized under growth-stress conditions (e.g. glutamate, an alternative source of nutrients excreted under growth-stress conditions, i.e. poor growth performance [5]). Another possibility would be the interspecific activation of the transporter system: A activates b's transport system and therefore facilitates/enhances the uptake of B (e.g. arabinose-activated synthesis of transporters that take up also galactose [6]). Or even the possibility to take up byproducts from other strains that prevent futile cycles and therefore improve growth in the "target" strain.

S.IV Parametrization

The extremes of the interaction function reveal how dramatic the effect of the producer strain, e.g. c, is upon the target strain's growth. Choosing $R_{top} = 0.75$ and $R_{min} = 1 - R_{top}$, for example, phenotype a can only reach maximal levels, μ_{max}, if $R_a(y_c) = 1$, but maintains a minimal growth even if the biotic driver is not strong enough to trigger interaction.

The choice of focal organism and physical environment (see Table 1) leaves only k_R and y_{ref} as free parameters. The latter indicates when the biotic driver triggers non-trivial interaction strengths (i.e. y such that $R \ncong R_{min}$ and $R \ncong R_{max} = R_{top} + R_{min}$), while k_R represents the susceptibility of the target strain or, in the case of a pairwise biotic driver (e.g. Eq.(6)), the degree of asymmetry between the two interacting strains that influences the dynamics of the target strain.

Following the exploratory method described below, we can find the (y_{ref},k_R) that give rise to RQ dynamics, at least for cases in which the driver depends only on the producer strain.

S.V Exploratory method to find the RQ

In some cases, it is possible to explore the parameter space by mapping the non-transitive cycle into a recursion for each strain, which facilitates a tentative prediction of the pairs (k_R, y_{ref}) for which RQ dynamics emerge. When the biotic driver depends only on the producer strain (e.g. Eq.(5)), the (negative) influence of a over b is qualitatively similar to the (negative) influence of c over a, and the whole non-transitive cycle can be qualitatively summarized as the effects of a over itself (see Fig.S2), $R_a(y_a(t))$. Thus, given an initial value for R_a, we calculate the associated ESS using Eqs.(S5); then, we calculate accordingly the new y_a using, e.g. Eq.(5), which in turn will determine a new value for R_a following Eq.(4), and so on. If such iteration leads to a stationary value, the pair (k_R, y_{ref}) potentially provides stasis for the complete 3-strain system; otherwise, sustained oscillations indicate potential RQ dynamics (see, e.g. Fig.S3 right).

On the other hand, the multi-strain dependence of y for pairwise drivers prevents a meaningful definition of the recursion $R_a(y_a)$, and therefore the exploratory method cannot be used to find the appropriate (k_R, y_{ref}) that enable RQ dynamics. We observed, however, RQ dynamics for all such pairwise drivers after generically setting $y_{ref} = 1$ and $k_R = 10$ in these cases.

S.VI Explicit functional forms for the driver

In the main text, we assume a positive relationship between the interaction strength R and its driver y (see Fig.S1), which in turn is negatively correlated with growth performance (see previous section). With this in mind, let us now enumerate a suite of possible forms for the driver that could represent such an interaction. Given the simplicity of our system, any interaction needs to include necessarily either the main traits and/or resources, which means that they will form part somehow of the biotic driver for the interaction strength. *i) Strain-specific performance driven factor*: In this group we can find cases in which the biotic factor that drives the interspecific interaction depends singly on the producer strain's performance. Because a bad performance translates into a smaller ratio of the inhibiting byproducts, the first option for the functional form for y is provided by Eq.(5), showing a positive correlation with K. We can also consider other definitions for "bad performance", for example defined as the need to increase the uptake rate potential to maintain the same growth rate; in this case, if a is the target strain and c the producer strain, y would be:

$$y_c = \frac{\mu_{max_c}}{\mu_{max_{c_{ESS}}}(R=1)}. \tag{S7}$$

where the normalization factor is, in this case, the maximum uptake rate in the best possible scenario for the producer strain ($R = 1$). Another valid normalization factor could be the reference value used for the trade-off, μ_{ref}. This choice does not affect qualitatively our results.

An additional definition for bad performance considers low affinity for the primary resource. Affinity measures the efficiency of the uptake process. Therefore, a poor affinity of c for C translates into poor growth performance and therefore increased inhibitor ratio hindering a's growth. Thus, there should be a negative correlation between affinity and

the driver, y. Defining affinity as the ratio of maximum uptake rate and half-saturation constant [7]:

$$y_c = \frac{K_c}{\mu_{max_c}} \left(\frac{K_{c_{ESS}}(R=1)}{\mu_{max_{c_{ESS}}}(R=1)} \right)^{-1}, \tag{S8}$$

where we used the link between uptake and growth to express y_c in terms of growth traits. Because we use as a normalization factor the ESS value for the affinity for $R = 1$, the yield parameter does not appear in this expression.

ii) Relative-performance driven factor: A plausible driver of the interspecific interaction could be relative growth performance, as opposed to individual performance as introduced above (see main text).

Thus, the expressions for y depend, in this scenario, on the traits of both the producer and target strains (e.g. c and a, respectively). In the "negative interaction" scenario necessary for the non-transitive cycle above, the inhibitory effect of c on a is less dramatic if a's growth performance is good. Therefore, if we represent growth performance with the half-saturation constant, the pairwise interaction driver takes the form provided by Eq.(6). If, on the other hand, we represent growth performance using the potential maximum uptake rate:

$$y_c = \frac{\mu_{max_c}}{\mu_{max_a}}, \tag{S9}$$

Finally, if we use nutrient affinity as a proxy for performance:

$$y_c = \frac{K_c}{\mu_{max_c}} \left(\frac{K_a}{\mu_{max_a}} \right)^{-1}. \tag{S10}$$

For such drivers, there is no need for normalization factor to compare results across cases.

iii) Resource-concentration driven factor: In all the cases above, we focus on growth-inhibiting byproducts. If, instead of ratios, it is individual inhibitor concentration that influences the interaction, other factors such as population density can drive the interaction across strains:

$$y_c = \frac{N_c}{N_{c_{ESS}}(R=1)}, \tag{S11}$$

Other possibilities are related with the limiting nutrient being directly the inhibitor for the target strain (e.g. C limiting a's growth), for example:

$$y_c = \frac{[C]}{[C]_{ESS}(R=1)} \tag{S12}$$

or the classic mathematical representation for nutrients that act as (non-competitive) inhibitors:

$$y_c = \frac{[C]}{K_a}. \tag{S13}$$

This expression gauges how available the inhibiting resource C is with respect to how efficient is a growing on its own nutrient. Finally, in terms of relative resource availability or relative biomass:

$$y_c = \frac{[C]}{[A]} \tag{S14}$$

$$y_c = \frac{N_c}{N_a}. \tag{S15}$$

As explained in the main text, however, the timing of changes in any driver in which concentration (or biomass) participate prevents the emergence of RQ dynamics, due to the short reaction time of the cells allowing the strains to acclimate ecologically without the need to rely on long-term evolutionary adaptation.

S.VII Biodiversity

In addition to monitoring the number of phenotypes per strain, we characterized genetic diversity by keeping track of the phenotype variability within each strain. To this end, we measured the standard deviation and inter-quartile range associated with the intraspecific trait distribution, for which we used the classic definitions [8]. We also measured the Shannon index (used in ecology to measure biodiversity), defined as:

$$I_{Sh_a}(t) = -\sum_{i=1}^{S_a} f_i \log(f_i) \tag{S16}$$

where f_i is the relative frequency of phenotype i within strain a, i.e. $f_i = \frac{N_i}{\sum_i N_i}$. The three indicators of biodiversity, I_{stdev}, I_{IQR}, and I_{Sh}, provided qualitatively-similar results to those shown in Fig.3.

S.VIII Additional results

ESS as a function of R

Fig.S3 shows that the interspecific interaction between strains alters the location of the minimum for resource requirement at the stationary state (a measure of competitive ability [2]); this minimum (which corresponds to the ESS, see S.II), is negatively correlated with R. A negative correlation can be also observed for the ESS value for the adaptive trait as a function of R (Fig.1, upper left). Importantly, these results are independent from the shape for the interaction function, R. Plots like Fig.1 (upper left) can help us determine the range of the changes in the ESS expected for a specific interaction strength interval. The range for the amplitude increases with the dilution rate (although increasing w decreases feasibility, S.II). The smaller the range is, the smaller the amplitude of oscillations and therefore the closer the resulting long-term behavior is to stasis.

Stasis

In the complete model, the stasis regime is highly nontrivial, as it results from the interaction between the three strains, each with a potentially different $R(t)$ and, therefore, each with a potentially different ESS value for their adaptive traits. In Fig.S4 (left panel),

we can see two different examples. In the inset, the three strains all reach the same ESS, which in turn agrees with the best possible scenario within the interval of possible R: the ESS associated with $R = 1$. Note that, in this case, the coupled evolutionary dynamics take the three strains to the (nontrivial) ESS whereas if we fixed R (i.e. constant forcing until the end of the experiment) the three strains would reach such state independently from each other.

In the main panel, we parametrized the trade-off functions with (arbitrary) strain-specific parameters, representing their growth on different nutrients. Due to the lack of information about other sugars' trade-offs, we assumed $\mu_{ref_a} = \mu_{ref}$, $\mu_{ref_b} = 2\mu_{ref}$, and $\mu_{ref_c} = 3\mu_{ref}$. As a result, the strains reach a different ESS. This quantitative differences are the only observed effect of changes in the trade-off function.
Regardless of the final outcome of the dynamics (i.e. RQ or stasis), the strain can be represented by the dominant at any time (see Fig.S4, right panel). Similarly, in the laboratory, sampling each strain will most probably result in obtaining the most abundant (i.e. dominant) phenotype.

One-strain recursion and interaction delay

As mentioned above, the recursion $R_a(y_a)$, i.e. the effect of a over itself, can summarize at least qualitatively the non-transitive cycle. When the same two R^{hi} and R^{lo} are visited by all strains, like in our system, the equivalence is also quantitative. As Fig.S2 points out, in the non-transitive cycle the effect of a over b is qualitatively similar to that of c over a; if each strain visits only the same two values for R (R^{lo} and R^{hi}) every cycle, and those two values agree for all strains, then the effect of a over b is also quantitatively similar to that of c over a, and we can map the cycle exactly into the effect of a over itself.
This recursion is meaningful when the driver depends on only the producer strain. For all the cases in which the biotic driver depends on the performance of one single strain (drivers given by Eqs.(5), and Eq.(S7) and (S8)), the $R_a(y_a(t))$ iteration predicts reliably the emergence of RQ or stasis in the complete model (e.g. Fig.S3, right). However, if the biotic driver depends on any of the rapidly-changing variables such as nutrient availability or population number (Eq.(S13)-Eq.(S15)), the R function changes equally frequently and $R_a(y_a(t))$ fails to predict the evolutionary outcome: oscillations are observed in the yellow regions predicted by the recursion, but only in the ecological variables and not in the adaptive traits, which reach an ESS.

This lack of a sufficient delay is also the reason why a one-strain system cannot show RQ dynamics with our setup, but the one-strain recursion $R_a(y_a)$ is able to predict when the 3-strain system does. Without the complete non-transitive cycle, parametrizations in the yellow areas will give rise to R^{lo} and R^{hi} that are, in one-strain cases, very close to each other (the resulting distribution for R or that of the adaptive trait are, effectively, unimodal as opposed to Fig.1, lower-left panel); the two "environmental conditions" between which the strain switches are therefore very similar, and the two potential dominant phenotypes are present at all times. Thus, alternation, i.e. oscillations occur artificially often and the strain converges to stasis.

Lack of ecological oscillations

As mentioned in the main text, the temporal behavior of the strains' population densities does not show a clear oscillatory trend or synchrony. Indeed, Fig.S5 shows that there is no periodicity in the changes for either the total population density or the dominant's density, whose dynamics are irregular but not oscillatory. Moreover, the increase in one strain's density does not necessarily lead to a decrease in the other two, nor does the number of cells reach almost negligible values like described in other RQ models [9]. The fact that the non-transitive cycle is driven by traits (i.e. evolution), and strains alternate between ESSs, explains why oscillations in the population densities are not needed to maintain the RQ.

Evolutionary rescue

Fig.S6 (left panel) shows that, during the initialization period, the number of phenotypes per strain increases monotonically. However, when the RQ regime is reached, the associated oscillations in the evolutionary lag lead to oscillations in the number of phenotypes, as peaks in lag trigger multiple phenotype extinctions whereas low lag allows for the accumulation of dominant-related phenotypes.

For sufficiently-high evolutionary lag values, the focal strain's biodiversity may not be high enough to "respond" to such a sudden environmental change, which drives the strain to extinction (Fig.S6, right). These cases can be avoided by introducing a new phenotype close to the new evolutionary target thus reducing the lag ("evolutionary rescue"). See main text for further discussion.

Alternative R functions

We tested the dependence of the RQ emergence on the functional form chosen for the interspecific interaction. To this end, we replaced Eq.(4) by the linear function $R = k_R\,(y - y_{ref})$, where there is no upper limit but we establish a lower limit ($R \geq R_{min}$ for any y, with R_{min} fixed such that $R_{min} \geq 0$).

With this linear functional form, we studied the case in which the biotic driver depends on the affinity of the producer strain, Eq.(S8) . The simplified one-strain scenario predicts evolutionary oscillations in a wide region of the parameter space; the 3-strain system shows large lag periods in that region that lead easily to the collapse of the population (results not shown). RQ dynamics emerge, however, when evolutionary rescue is included to perpetuate evolutionary oscillations.

Symbol	Description	Units	Value/Range
N_i	Population density for phenotype i	$cells \cdot L^{-1}$	Ecological variable
μ_{max_i}	Maximum growth rate phenotype i	d^{-1}	Evolutionary variable
K_i	Half-saturation constant phenotype i	$g \cdot L^{-1}$	Evolutionary variable
$[A]$	Concentration for nutrient A	$g \cdot L^{-1}$	Ecological variable
$[A]_{input}$	Input of nutrient A in the chemostat	$g \cdot L^{-1}$	$400 \cdot 10^{-6}$
R_a	Interspecific interaction function for strain a	–	Eco-evolutionary variable
y	Biotic driver for the interspecific interaction	Depending on choice	Eco-evolutionary variable
y_{ref}	Modulator for biotic driver in the R function	Same as y	0.5-5
k_R	Steepness for the R function	–	1-50
w	Chemostat dilution rate	d^{-1}	4.8
Y	Cell yield factor	$cell \cdot g^{-1}$	$4.96 \cdot 10^{12}$
μ_{ref}	Reference max. growth rate for trade-off function	d^{-1}	32.4
K_{ref}	Reference half-saturation constant for trade-off function	$g \cdot L^{-1}$	$5.5 \cdot 10^{-6}$
R_{top}	Added to R_{min}, max. value interaction function	–	0.75
R_{min}	Min. value interaction function	–	0.25
p_{mut}	Mutation rate	$mutations \cdot generation^{-1}$	10^{-6}

Table S1: Table of parameters and variables in the system. The first group are phenotype-specific, the second group, strain-specific, the third group depend on the type of biotic driver, and the last group are common to all phenotypes. Typical *E. coli* values for parameters in the last group taken from [1, 10] and our own laboratory reference values.

References

[1] Wirtz, K.W. A generic model for changes in microbial kinetic coefficients, *J. Biotech.* **97**, 147-162 (2002).

[2] Tilman D. *Resource Competition and Community Structure* (Princeton University Press, 1982).

[3] Dercole, F. & Rinaldi, S. *Analysis of Evolutionary Processes: the Adaptive Dynamics Approach and its Applications* (Princeton University Press, 2008).

[4] Commichau, F.M., Gunka, K., Landmann, J.J. & Stülke, J. Glutamate metabolism in *Bacillus subtilis*: gene expression and enzyme activities evolved to avoid futile cycles and to allow rapid responses to perturbations of the system, *J. Bacteriol.* **190**, 3557-3564 (2008).

[5] Burkovski, A., Weil, B. & Krämer, R. Glutamate excretion in *Escherichia coli*: dependency on the relA and spoT genotype, *Arch. Microbiol.* bf 164, 24-28 (1995).

[6] Krispin, O. & Allmansberger, R. The *Bacillus subtilis* AraE protein displays a broad substrate specificity for several different sugars, *J. Bacteriol.* **180**, 3250-3252 (1998).

[7] Healey, F.P. Slope of the Monod Equation as Indicator of Advantage in Nutrient Competition, *Microb. Ecol.* **5**, 281-286 (1980).

[8] Mendenhall, W., Beaver, R.J., & Beaver, B.M. Introduction to probability and statistics. Belmont, CA: Brooks/Cole, Cengage Learning (2009).

[9] Rabajante, J.F., Tubay, J.M., Uehara, T., Morita, S., Ebert, D., & Yoshimura, J. Red Queen dynamics in multi-host and multi-parasite interaction system, *Sci. Rep.* **5**, 10004 (2015).

[10] Lendenmann, U., Snozzi, M., & Egli, T. Kinetics of the simultaneous utilization of sugar mixtures by *Escherichia coli* in continuous culture, *App. Env. Microbiol.* **62**, 1493-1499 (1996).

Supplementary figures

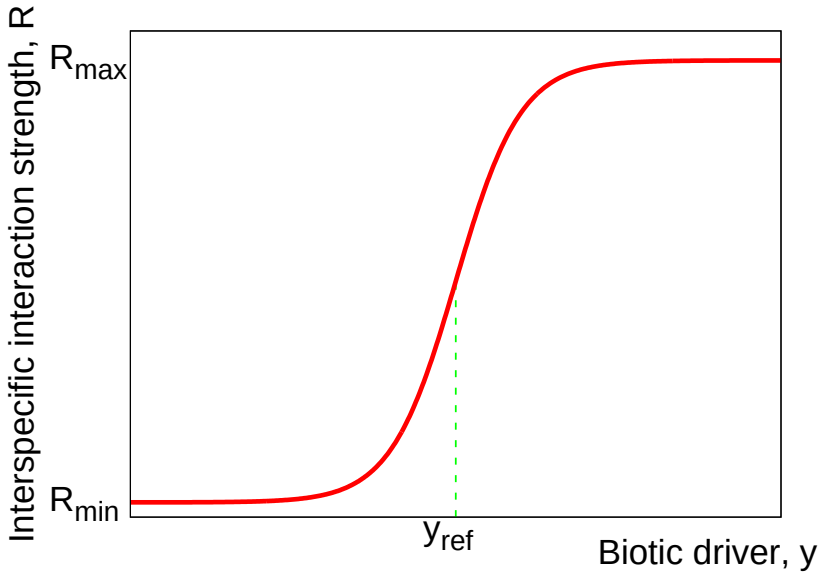

Figure S1: Interspecific interaction strength, R, as a function of the biotic driver value, y, as determined by Eq.(4).

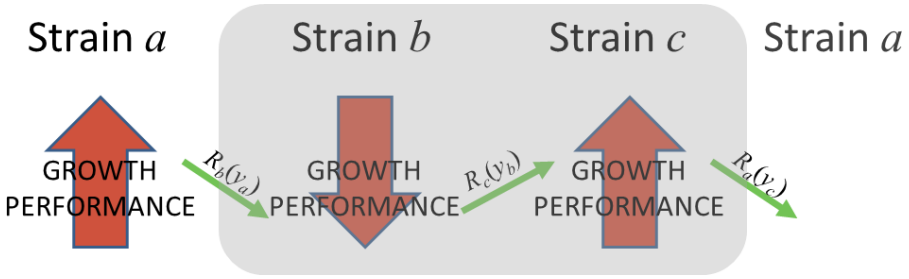

Figure S2: Non-transitive cycle in which evolutionary changes in growth performance for each strain (larger, red arrows) alter the interspecific interaction, change encoded with R (smaller, green arrows).

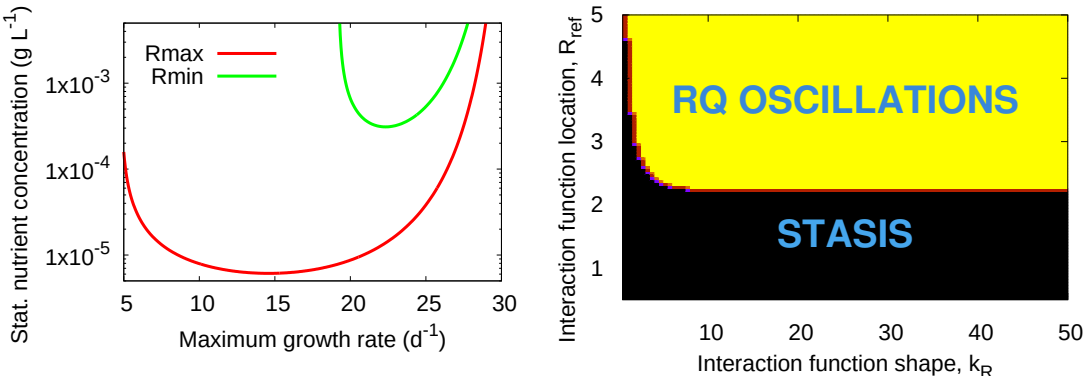

Figure S3: Left: Dependence of the resource requirement at the stationary state (Eq.(S2)) on the maximum growth rate, assuming a constant interspecific interaction strength R fixed at two specific values ($R_{max} = 1$ and $R_{min} = 0.25$). Right: Parameter space showing the potential for RQ dynamics (yellow) and stasis (black) for the K-dependent driver, Eq.(5).

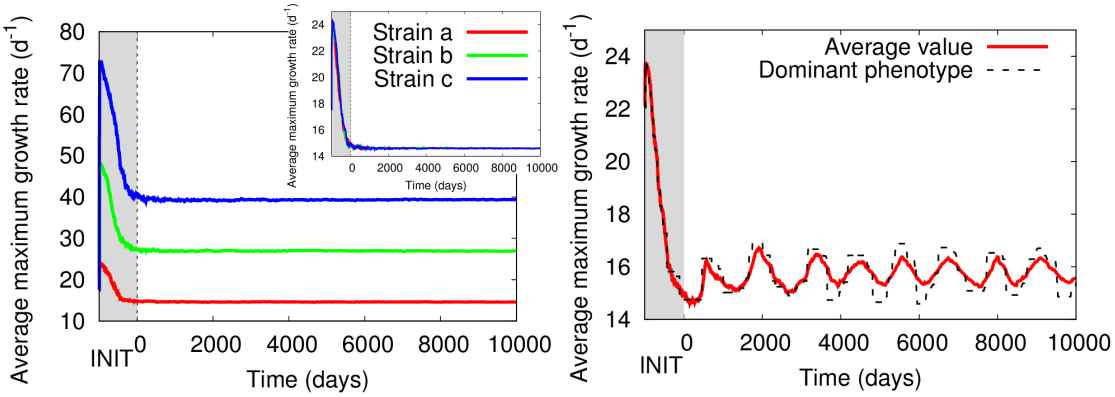

Figure S4: Stasis emerging from the dynamics with three strains when $k = 10$ and $y_{ref} = 1.5$; the three strains interact dynamically until they reach the strain-specific ESS given by Eq.(S5) with μ_{ref} increased by a strain-specific factor (see main text). Inset: Stasis resulting from using the same trade-off parameters for all strains, which results in the same ESS. Right: Strain a evolutionary dynamics for the RQ case in Fig.1, considering the average value for the adaptive trait, μ_{max} (red line) and value for the dominant phenotype (black dashed line).

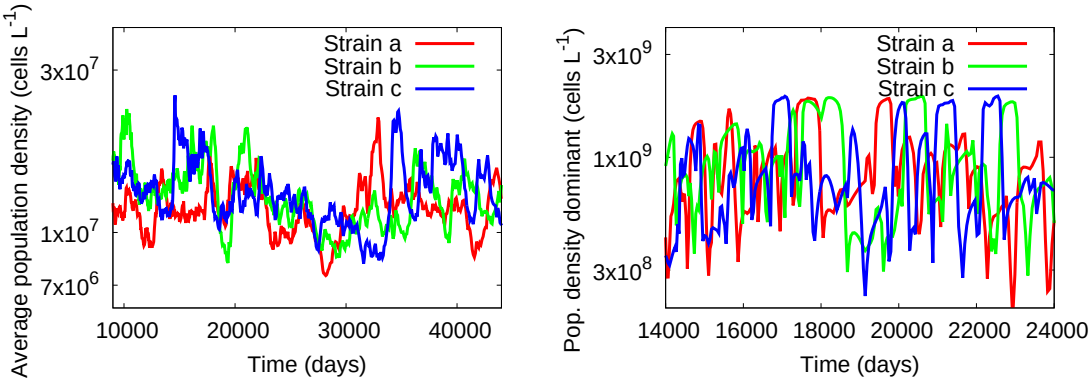

Figure S5: Left: Temporal behavior of the average population density for each strain. Right: Temporal behavior of the population density for each strain's dominant phenotype.

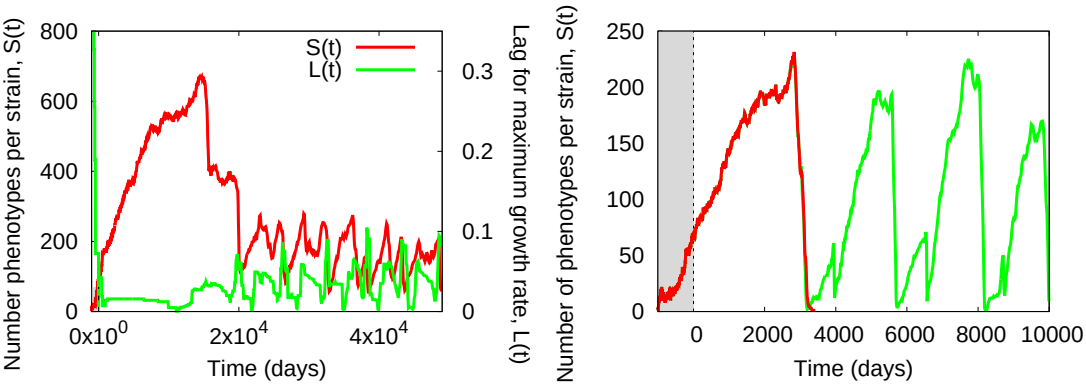

Figure S6: Dynamics for the number of phenotypes within strain a. Left: Number of phenotypes (red line) and associated lag (in this case, for μ_{max}, green line) as a function of time, showing the coincidence of peaks in lag and dips in $S(t)$; the biotic driver is the ratio of maximum growth rates (Eq.(S9)) with $k_R = 10$ and $y_{ref} = 1$. Right: Example of crashing simulation (red line) and "rescued" simulation (green line) for a driver described by Eq.(6) and same R parameters as left panel.